Atmos. Chem. Phys., 26, 13581–13593, 2026
https://doi.org/10.5194/acp-26-13581-2026

Atmospheric Chemistry and Physics
Open Access
EGU

Research article

Impacts of South Asian aerosol inflow over Mount Qomolangma on downstream cloud–precipitation processes through a long-range ice-crystal "seeding" effect

Xiangde Xu[1,★], Wenyue Cai[1,★], Tianliang Zhao[2], Changjun Yang[3], Kai Meng[4], Chong Wu[1], Na Dong[1,5], Yueqing Li[6], Shunjiu Wang[6], Wenqing Liu[7], Tianshu Zhang[7], Ga Zhuo[8], Shengjun Zhang[1], Bin Chen[1], Chunsong Lu[2], Jinghua Chen[2], Kai Yang[2], and Jianming Xu[9]

[1]State Key Laboratory of Severe Weather Meteorological Science and Technology, Chinese Academy of Meteorological Sciences, Beijing 100081, China
[2]Key Laboratory for Aerosol-Cloud-Precipitation of China Meteorological Administration, Nanjing University of Information Science and Technology, Nanjing 210044, Jiangsu Province, China
[3]Key Laboratory of Radiometric Calibration and Validation for Environmental Satellites, National Satellite Meteorological Center (National Centre for Space Weather), China Meteorological Administration, Beijing 100081, China
[4]Hebei Key Laboratory of Meteorology and Modern Economy, Hebei Provincial Institute of Meteorological Sciences, Shijiazhuang 050021, China
[5]Department of Atmospheric and Oceanic Sciences & Institute of Atmospheric Sciences, Fudan University, Shanghai 200438, China
[6]Heavy Rain and Drought-Flood Disaster in Plateau and Basin Key Laboratory of Sichuan Province, Chengdu Institute of Plateau Meteorology, China Meteorological Administration, Chengdu 610072, China
[7]Key Laboratory of Environment Optics and Technology, Anhui Institute of Optics and Fine Mechanics, Chinese Academy of Sciences, Hefei 230031, China
[8]Mêdog National Climate Observatory, Mêdog 860700, China
[9]Shanghai Meteorological Center, Shanghai Meteorological Service, Shanghai 200030, China
★These authors contributed equally to this work.

Correspondence: Wenyue Cai (caiwy@cma.gov.cn) and Tianliang Zhao (tlzhao@nuist.edu.cn)

Received: 31 May 2026 – Discussion started: 23 June 2026
Revised: 2 September 2026 – Accepted: 2 September 2026 – Published: 29 September 2026

Abstract. Mount Qomolangma (MQ) serves as a natural laboratory for investigating aerosol–cloud–precipitation interactions over the Tibetan Plateau (TP). Using satellite and comprehensive ground-based observations, we identify pronounced ice-cloud activation associated with transported exogenous aerosols. Under different large-scale atmospheric circulation regimes, ice-phase cloud activated over MQ can be efficiently transported downstream through distinct pathways, exerting a pronounced ice crystal seeding effect on cloud–precipitation conversion. The spatial patterns of these downstream pathways are highly consistent with regions of enhanced ice-phase occurrence, precipitation, and upper-tropospheric latent heat release. This study provides new insight into the downstream impacts of aerosol transport through ice seeding for cloud precipitation. The findings highlight the important role of aerosol-induced ice-phase processes in modulating cloud and precipitation systems over the "Third Pole" and its downstream regions, with significant implications for understanding downstream extreme precipitation and environment change under South Asian increasing anthropogenic influences.

1 Introduction

The evolution of precipitation is complex and occurs in various forms, influenced not only by multiple physical processes – such as vertical motion within clouds, liquid water production, turbulent structures, and cloud lifetimes – but also by the characteristics of aerosol loading (Twomey et al., 1984; Levin and Cotton, 2009; Xu et al., 2025). Theoretically, aerosols exert the significant influence on both the development of clouds and the formation of precipitation from the macrophysical and microphysical perspectives (Zhang et al., 2017; Zhou et al., 2017; Zhao et al., 2024). Aerosols can act as cloud condensation nuclei (CCN) or ice-nucleating particles (INPs), altering cloud microphysical properties and precipitation processes (Twomey, 1977; Penner et al., 2001; Rosenfeld et al., 2014; Zhao et al., 2025). However, for a long time, the role of anthropogenic aerosols in modulating cloud and precipitation has long remained a contentious issue in climate science, with substantial evidence supporting both enhancement (Khain et al., 2005; Fan et al., 2018) and suppression (Qian et al., 2009; Liu et al., 2011; Guo et al., 2016; Liu et al., 2020b) effects on precipitation. Regional studies further emphasize such complexity (Giorgi et al., 2002; Menon et al., 2002).

Over the Tibetan Plateau (TP), aerosol–cloud–precipitation interactions are particularly important because externally transported aerosols can be lifted rapidly by strong topographic and convective ascent (Xu et al., 2025). Mounting evidence suggests that the southern slopes of the Himalayas now serve as a major transport pathway and sensitive receptor zone for aerosols originating from South Asia (Hindman and Upadhyay, 2002; Ramanathan et al., 2005; Huang et al., 2007; Lawrence, 2011; Ming et al., 2013; Liu et al., 2015; Cong et al., 2015; Kang et al., 2019; Li et al., 2020; Liu et al., 2020a; Wang et al., 2020; Zhao et al., 2020). This implies that an issue of aerosols influencing cloud properties have emerged as a new challenge for research on the role of the TP in climate change. The Mount Qomolangma (MQ) as a natural laboratory for investigating aerosol–cloud–precipitation interactions over the TP (Xu et al., 2025). During the MQ aerosol–cloud–precipitation integrated vertical observation campaign, Xu et al. (2025) showed that, during the Indian summer monsoon, aerosols transported from South Asia exerted a pronounced activation effect on cloud and precipitation processes. Under dynamically forced lifting conditions, enhanced aerosol loading suppressed and delayed weak precipitation over MQ while promoting more vigorous cloud development, ultimately resulting in increased precipitation on the northern slope. The synergistic interaction between the thermodynamic–dynamic forcing over MQ and aerosol activation favored the development of deep convection associated with precipitation on the northern slope. Aerosol activation also enhanced cloud development. Convective-cloud development over the MQ region was found to be more responsive to aerosol than to atmospheric moisture conditions, suggesting that aerosol activation plays a key role in regulating the evolution of convective clouds (Xu et al., 2025). From thermodynamic and dynamic perspectives, Xu et al. (2025) further elucidated the relationships between AEC levels over MQ and the associated atmospheric dynamic and thermodynamic conditions, as well as the complex relationships between heavy precipitation and meteorological factors, including vertical motion, water vapor, humidity, and aerosols. High-aerosol-loading episodes were characterized by a stronger apparent heat source (Q_1) than low-aerosol-loading episodes, thereby enhancing ascending motion over the southern slope of MQ.

Under these distinct dynamic and thermodynamic conditions, the occurrence frequencies of ice-phase and mixed-phase clouds were significantly higher during high-aerosol-loading episodes than during low-aerosol-loading episodes (Xu et al., 2025). Aerosols acting as CCN and INPs may alter cloud droplet activation, promote heterogeneous ice nucleation, and modify the partitioning among liquid, supercooled-liquid, mixed-phase, and ice-phase clouds (Zhu et al., 2024). A small subset of atmospheric aerosol particles can act as INPs and initiate heterogeneous ice formation in ice-phase clouds through immersion, deposition, contact, or condensation freezing. Mineral dust and soot particles are regarded as the primary atmospheric INP types. Over the TP and its surrounding regions, transported soot and dust aerosols have been linked to variations in ice-crystal effective radius, ice water content, cloud optical properties, and cloud-phase partitioning (Liu et al., 2019). Once primary ice crystals are generated, depositional growth, riming, the Wegener-Bergeron-Findeisen process (Wegener, 1911; Bergeron, 1935; Findeisen, 1938), and secondary ice production can further amplify cloud glaciation and modify the partitioning between liquid and ice water (Murray et al., 2012). Nevertheless, aerosol concentration alone does not directly represent INP abundance, and the observed aerosol–ice-cloud relationship may also be affected by temperature, humidity, vertical motion, and cloud dynamics (Zhu et al., 2024; Xu et al., 2025). Atmospheric aerosols interact with clouds through tightly coupled microphysical, radiative, thermodynamic, and dynamical processes. Vertical motion, moisture availability, temperature and large-scale circulation are meteorological factors that collectively determine whether elevated aerosol loading stimulates or inhibits cloud and precipitation development. Therefore, the ice-phase clouds could be interpreted as the combined result of aerosol-mediated ice nucleation and favorable thermodynamic and dynamical conditions, rather than as an aerosol effect alone. These interactions are highly nonlinear and depend strongly on cloud type, cloud evolutionary stage, and the surrounding meteorological environment (Intergovernmental Panel on Climate Change, 2023). Despite these impacts, the intricate interactions between aerosol and cloud microphysics make the effects of aerosol on precipitation poorly understood (Levin and Cotton, 2009), and understanding of aerosol–cloud–precipitation interactions over the TP and their downstream impacts remains particularly limited.

As the roof of the world, the TP acts as a vast engine, driving the nearby movements of water vapor, clouds, and aerosols (Kang et al., 2019; Liu et al., 2020a). The TP shows prominent transport characteristics of cloud systems and water vapor over itself and surrounding regions. Such eastward transport effect is vital to the formation of precipitation processes and even floods in downstream eastern China (Xu et al., 2001, 2002: Xu and Chen, 2006; Miao et al., 2002; Zhuo et al., 2002; Wan et al., 2017). Therefore, under favorable thermodynamic and dynamic conditions, aerosol-influenced cloud particles and ice crystals may be transported downstream, potentially affecting cloud-to-precipitation conversion beyond the aerosol source region. Nevertheless, previous studies have only examined the effects of aerosols over the TP and its surrounding areas on local precipitation (Jiang et al., 2023; Ying et al., 2023). without considering the possible upstream-downstream linkage effects between the plateau and eastern China induced by the transport effect of the TP.

As part of the Second Tibetan Plateau Scientific Expedition and Research Program (STEP), a comprehensive vertical observation experiment focusing on aerosol–cloud–precipitation interactions was carried out in the MQ region (Xu et al., 2025). This observational framework combines ground-based aerosol lidar measurements, X-band dual-polarization weather radar observations for mesoscale weather systems, routine surface meteorological observations and satellite observations for the first time (Ma et al., 2023; Xu et al., 2025). Leveraging these coordinated measurements, we herein explore the impacts of South Asian aerosol inflow over MQ on downstream cloud-precipitation processes. In particular, the activation of ice-phase clouds by transported aerosols and the subsequent long-range downstream transport of ice nuclei may exert a “seeding” effect, whereby ice crystals enhance cloud–precipitation conversion processes far from their source regions. Such mechanisms could alter latent heat release, cloud dynamics, and precipitation patterns in downstream areas of East Asia. Consequently, investigating the pathways and mechanisms through which aerosol-activated ice clouds influence downstream cloud–precipitation systems holds fundamental scientific significance and practical relevance in the context of climate change and increasing anthropogenic activities.

2 Data and methods

2.1 Observation and Reanalysis

1. A ground-based aerosol lidar system manufactured by the Anhui Institute of Optics and Fine Mechanics, Chinese Academy of Sciences, was deployed at the MQ site to conduct continuous observations of aerosol extinction coefficients (AEC) during July 2018 and July 2019 (Xiang et al., 2021; Ma et al., 2023). The AEC was retrieved using the Fernald inversion method (Fernald, 1984), and cloud contamination was removed using an empirical threshold-based cloud-screening algorithm (Liu and Sugimoto, 2002). Detailed quality-control procedures follow those described by Xiang et al. (2020). In this study, aerosol conditions were classified based on daily mean AEC values at the MQ site (Xu et al., 2025). Days with AEC $\geq 0.025\,\mathrm{km}^{-1}$ were defined as high-aerosol-loading events, whereas days with AEC $< 0.025\,\mathrm{km}^{-1}$ were classified as low-aerosol-loading events for both July 2018 and July 2019 (Table S1 in the Supplement).

2. An X-band dual-polarization weather radar, provided by the Institute of Plateau Meteorology, China Meteorological Administration, Chengdu, was operated at the MQ site during July 2019 (Ma et al., 2023). The radar data underwent comprehensive quality-control procedures, including ground-clutter suppression, noise-bias correction of correlation coefficients and differential reflectivity, differential phase filtering, estimation of differential propagation phase shift, and attenuation correction for reflectivity and differential reflectivity (Xiao et al., 2012; Wang et al., 2019). These processed radar observations were used to characterize convective intensity and precipitation-related microphysical features and to examine their relationships with aerosol loading and cloud-phase variations.

3. Hourly full-disk cloud-phase products from the FengYun-4A Advanced Geosynchronous Radiation Imager (FY-4A/AGRI), provided by the National Satellite Meteorological Center of China, were used to identify cloud-phase distributions. The data are provided in a nominal projection with a spatial resolution of 4 km at nadir. Cloud-phase statistics for July 2018 and July 2019 were derived to examine the upstream–downstream relationships between aerosol loading, cloud-phase occurrence, and precipitation under high- and low-aerosol conditions at the MQ site.

4. Monthly aerosol optical depth (AOD) data at 550 nm from the MODIS Combined Dark Target and Deep Blue Collection 6.1 product were used to characterize long-term aerosol distribution and trends over South Asia and East Asia during July 2000–2020. The data have a spatial resolution of $1^\circ \times 1^\circ$, which is particularly suitable

for bright surfaces such as plateaus, deserts, and arid regions (Levy et al., 2013; Sayer et al., 2014; de Leeuw et al., 2018).

5. Hourly and daily surface meteorological observations were obtained from the Data Sets of Surface Meteorological Elements in China released by the National Meteorology Information Center, China Meteorological Administration. These data were used to analyze precipitation variability and its relationship with aerosol and cloud-phase anomalies in downstream regions. To examine large-scale circulation patterns and latent heat distributions associated with different aerosol-loading conditions, hourly and monthly meteorological reanalysis data for July 2018 and July 2019 were obtained from the European Centre for Medium-Range Weather Forecasts. The data have a horizontal resolution of $0.25° \times 0.25°$ and were used to characterize atmospheric circulation structures and thermodynamic anomalies linked to aerosol-induced cloud and precipitation responses.

2.2 Design of aerosol transport simulation

The FLEXPART particle diffusion model was employed (version 9.0) (Stohl et al., 2005), designing to take the FNL reanalysis data as the driving field, forward-trajectory of the aerosol particle swarms of high-concentration aerosol processes over the MQ from 9 to 11 July 2018 were simulated. The particle swarms were initially placed at (28–29° N; 86–88° E) at drop heights of 4426–7000 m a.s.l. Since only the physical transport process of aerosols and ice crystals in the atmosphere was focused on in this paper, the type of pollutants in the model was set as a tracer with the same density in dry air, which is not involved in the chemical reaction process of secondary aerosols in the atmosphere, considering the large amounts of primary sand dust and carbonaceous aerosols in the air south of the TP (Huang et al., 2007). The data of FNL (Final Operational Global Analysis) with a spatial resolution of $1° \times 1°$ from 2018, produced by the National Center for Environmental Prediction (NCEP)/National Center for Atmospheric Research (NCAR), was used as the driving field to simulate and synthesize the forward trajectories of the aerosol particle swarms of high-concentration aerosol processes over the MQ in July 2018.

3 Results

3.1 Aerosol–cloud phase relationships in deep convective systems over the MQ

Recently, the spatial correlation of the daily AOD with cloud properties and precipitation during both wet and dry monsoonal years indicated a positive association of relatively high aerosol concentrations with cloud vertical development and precipitation (Adhikari and Mejia, 2021). Satellite observations indicate pronounced AOD over South Asia and the Himalayan region, with a zonally elongated band of high correlation between South Asian aerosols and aerosol loading along the southern TP margin near MQ (Fig. 1a). This high-AOD belt, stretching from the South Asian plains to the Himalayan foothills, is commonly known as the Atmospheric Brown Cloud (Ramanathan et al., 2005; Zhao et al., 2020). Interannual variability in July AOD from 2000 to 2020 further reveals persistent and intensifying aerosol accumulation along the southern Himalayan slopes, originating from South Asia and showing a clear upward trend (Fig. 1b). These aerosols have been demonstrated to substantially influence cloud microphysical processes and precipitation patterns (Xu et al., 2025).

Relatively, the aerosol loading over the TP is much lower than those over other regions, thus leading to the more sensitive response of precipitation to aerosol-cloud interactions (Liu et al., 2022). Cloud and precipitation processes are easily affected in relatively clean atmospheric environments (Garrett and Zhao, 2006; Zhao et al., 2020). Previous studies have already revealed that absorbing aerosols over the TP have been proposed to directly affect monsoon rainfall through the elevated-heat-pump mechanism (Lau et al., 2008; Luo et al., 2020; Liu et al., 2022). During the Indian summer monsoon, low-level moist air masses originating from the Arabian Sea transport substantial aerosol loads across the Indian subcontinent and ascend along the southern slopes of the Himalayas toward MQ, supplying abundant CCN and INP essential for orographic cold-cloud precipitation. Observations reveal a positive correlation between aerosol concentration and the abundance of ice-phase hydrometeors in anvil clouds; the associated latent heat release from enhanced freezing further intensifies updrafts. Satellite-derived cloud-phase statistics demonstrate that under high aerosol loading, the occurrence frequencies of ice-phase, supercooled liquid, and mixed-phase clouds are 52.81 %, 20.68 %, and 16.34 %, respectively – compared to 35.71 %, 15.22 %, and 8.06 % under low aerosol loading. Conversely, liquid-phase clouds occur significantly more frequently under low aerosol conditions (13.98 %) than under high aerosol conditions (4.83 %) (Fig. 1c). Compared with water clouds, ice clouds are observed more frequently and are more significantly correlated with aerosols over the TP, which is consistent with prior observational and modeling evidence (Hua et al., 2020).

An integrated analysis of the diurnal cycles of aerosol extinction coefficients from lidar observations, maximum radar reflectivity from X-band dual-polarization radar, and cloud-phase frequencies further reveals that aerosol concentrations exhibit a statistically robust positive correlation exclusively with ice-phase and mixed-phase cloud occurrences – not with liquid- or supercooled liquid-phase clouds (Fig. 1d). Moreover, ice-phase and mixed-phase clouds display in-phase peak–trough relationships with the diurnal cycle of maximum radar reflectivity (Fig. 1e), indicating that these cloud types represent the dominant manifestation of

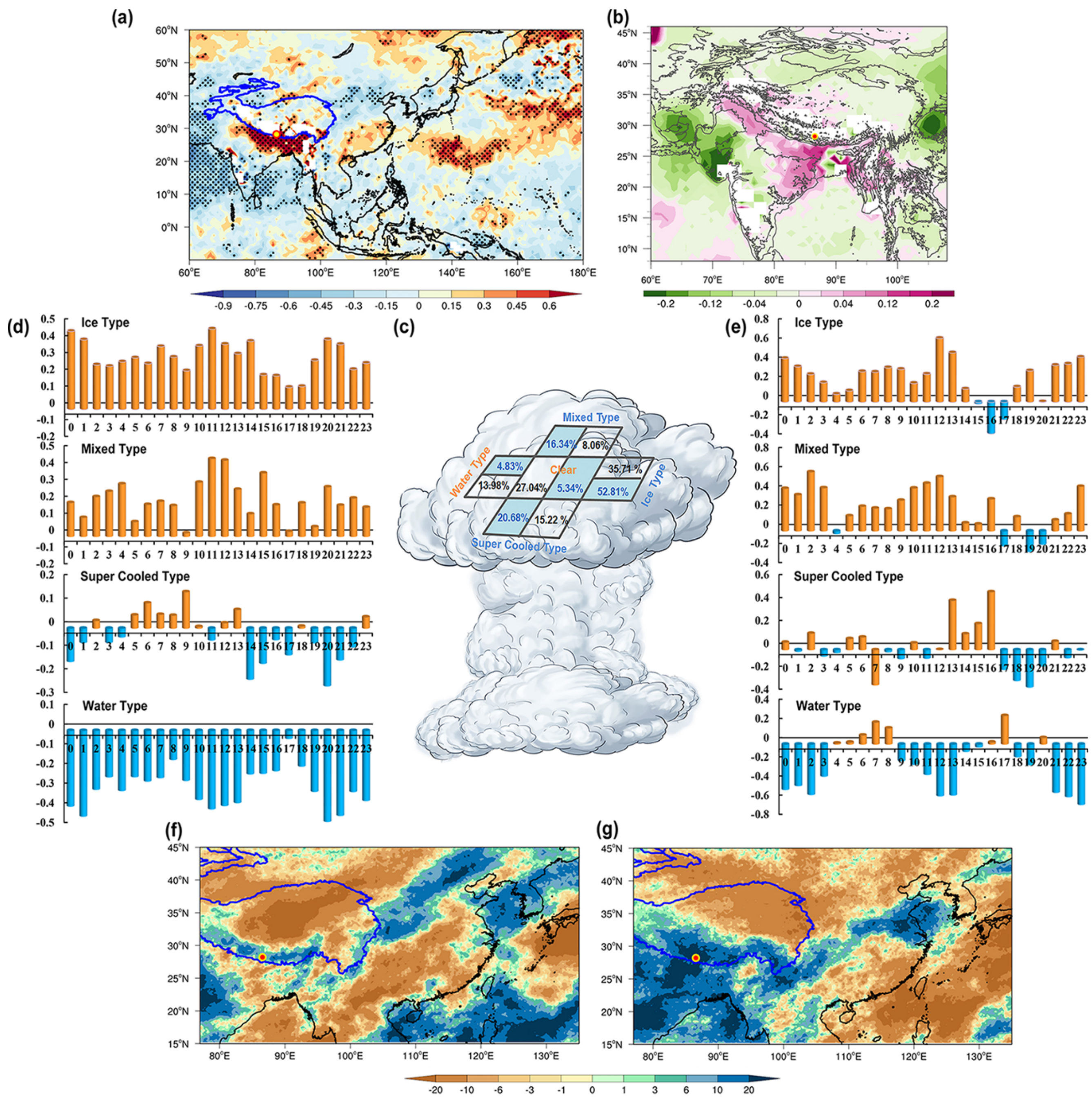

Figure 1. Aerosol distribution and cloud-phase responses over MQ: **(a)** Spatial correlation between AOD over the MQ region and East Asia during July 2000–2020, dotted regions indicate correlations statistically significant at the 90 % confidence level ($P < 0.1$, $n = 21$); **(b)** linear trends of July AOD over South Asia and the Himalayan region during 2000–2020; **(c)** percentage contributions of ice-phase, mixed-phase, supercooled liquid, and liquid clouds under high- and low-aerosol-loading conditions during July 2018 and July 2019; **(d)** diurnal variation in the correlation coefficient between lidar-derived aerosol extinction coefficient and cloud-phase occurrence ($n = 62$, July 2018 and July 2019); **(e)** diurnal variation in the correlation coefficient between maximum radar reflectivity from X-band dual-polarization radar and cloud-phase occurrence ($n = 31$, July 2019); **(f, g)** spatial distributions of daily ice-phase cloud-frequency anomalies (unit: %) under high- versus low-aerosol-loading for **(f)** July 2018 and **(g)** July 2019.

aerosol-induced deep convective activation. Aerosol concentrations significantly promote the formation of ice-phase and mixed-phase clouds in deep convective systems, whereas low aerosol concentrations favor the persistence of liquid-phase clouds. Under the combined effects of strong orographic lifting and enhanced thermodynamic forcing over MQ, aerosol facilitate the formation of additional ice clouds. The associated latent heat release enables more numerous and smaller cloud droplets to be lifted to higher altitudes, enhancing collision, riming, and aggregation processes among ice crystals and cloud droplets. High concentrations of carbonaceous aerosols, acting as efficient ice nuclei, preferentially activate convective clouds dominated by ice-phase and mixed-phase hydrometeors, thereby intensifying deep convection over MQ. This finding aligns with prior observational and modeling evidence showing that high aerosol loading enhances deep convective cloud invigoration and strengthens the heat source over MQ (Xu et al., 2025), thereby may further intensifying thermodynamic forcing on downstream cloud and precipitation systems.

3.2 Downstream transport pathways and cloud–precipitation responses

The Tibetan Plateau's unique dynamical characteristics (Xu et al., 2001, 2002; Xu and Chen, 2006; Zhuo et al., 2002; Wan et al., 2017; Kang et al., 2019; Liu et al., 2020a), acting as a quasi-stationary large-scale vortex, enable aerosol–cloud interactions to not only affect the local precipitation but also contribute to downstream precipitation. In July 2018, the downstream pathway of ice-phase and mixed-phase cloud-frequency anomalies associated with high- versus low-aerosol-loading extended from MQ along a southwest–northeast corridor toward the northeastern Tibetan Plateau and the Yellow River basin. In July 2019, the anomaly pathway associated with high- versus low-aerosol-loading extended predominantly eastward from MQ along the Yangtze River and Huai River basins. Figure 1f and g illustrate the banded upstream–downstream distributions of daily ice-phase and mixed-phase cloud-frequency anomalies under high versus low aerosol conditions for July 2018 and July 2019, respectively.

Variations in large-scale circulation patterns modulate the upstream–downstream impacts of high- versus low-aerosol-loading, giving rise to distinct downstream pathways of cloud-phase anomalies. In particular, downstream cloud-phase anomalies are dominated by ice-phase and mixed-phase clouds, rather than liquid or supercooled liquid clouds (Fig. S1). When numerous ice crystals form through vapor sublimation and the freezing of lofted cloud droplets, substantial latent heat is released, further intensifying convective development (Rosenfeld, 2006). Analysis of 300 hPa circulation anomalies and latent heat release anomalies under high- versus low-aerosol-loading conditions over MQ for July 2018 and 2019 reveals that the spatial distribution of latent heat anomalies (Fig. 2a, b) align closely with that of the pathways of ice-phase cloud-frequency anomalies (Fig. 1f, g). In July 2018 and July 2019, the spatial correlation coefficients between latent heat anomalies at 300 hPa (Fig. 2a, b) and ice-phase cloud-frequency anomalies (Fig. 1f, g) were 0.53 ($P < 0.001$) and 0.62 ($P < 0.001$), respectively. Compared with low aerosol conditions, high aerosol loading over MQ leads to notably stronger cloud–precipitation activation and more pronounced downstream effects. Precipitation anomalies also exhibit distinct downstream pathways. In July 2018, precipitation anomaly percentages form a southwest–northeast-oriented band extending toward the northeastern TP and the Yellow River basin, while in July 2019, the anomalies extend eastward along the Yangtze and Huai River basins (Fig. 2d, e). Analysis of 300 hPa circulation anomalies and latent heat release anomalies under high- versus low-aerosol-loading conditions over MQ for July 2018 and 2019 reveals that the spatial distribution of latent heat anomalies (Fig. 2a, b) exhibits broadly similar to that of the pathways of precipitation anomaly percentages (Fig. 2d, e). This reveals that high aerosol loading over MQ exerts a dual influence along downstream transport pathways: it enhances cloud ice–precipitation conversion through effective glaciation seeding, and it induces pronounced anomalies in upper-tropospheric latent heat release. Among these, INPs initiate heterogeneous ice nucleation in supercooled clouds (Lohmann and Feichter, 2005). Aerosol-enhanced deep convection over MQ propagates thermodynamic perturbations over long distances, driving coordinated ice-cloud development, cloud–ice interactions, and vertically distributed latent heat release across multiple tropospheric layers. Through this cascade, ice crystals serve as precipitation embryos that seed lower-level clouds and reorganize precipitation spatial patterns along climatically sensitive downstream corridors, ultimately reshaping regional cloud regimes and precipitation distributions over Eastern China (Fig. 2c). Furthermore, the contrasting downstream precipitation pathways between the two years underscore the critical role of background circulation patterns – such as the subtropical high and monsoon system configurations – in shaping aerosol-induced cloud–precipitation responses.

3.3 Seeding effects of aerosol-activated ice clouds on downstream precipitation

To further confirm the seeding effects of aerosol-activated ice clouds on downstream precipitation, we perform tracking analyses of upstream high-aerosol events to investigate their influences on downstream precipitation in the following three days, that is, the downstream precipitation-affected regions evolve continuously starting from the pollution day over the subsequent two days. As shown in Fig. 3, with the occurrence of upstream high-aerosol episodes, intense precipitation gradually develops over eastern downstream regions, and higher precipitation is observed. These heavy pre-

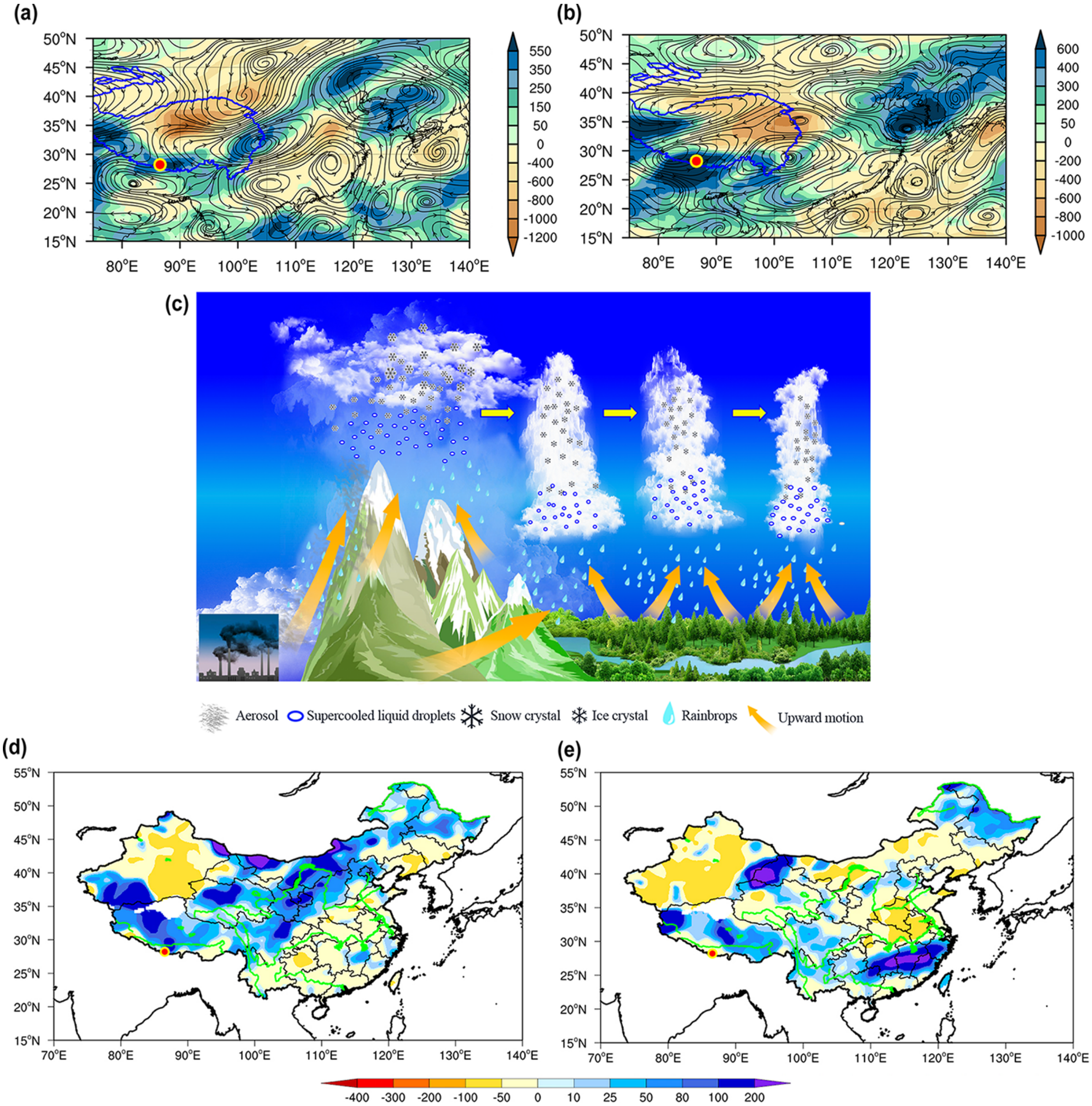

Figure 2. Downstream pathways of latent heat release and precipitation anomalies: **(a, b)** Anomalies in 300 hPa atmospheric circulation (first-order filtered) and latent heat release under high- versus low-aerosol-loading conditions over MQ for **(a)** July 2018 and **(b)** July 2019; **(c)** conceptual schematic illustrating the ice-nucleating role of externally transported aerosols in promoting ice-cloud–precipitation conversion and modulating downstream precipitation; **(d, e)** spatial distributions of precipitation anomaly percentages for **(d)** July 2018 and **(e)** July 2019.

cipitation belts align closely with the high-frequency downstream pathways of ice-phase and mixed-phase clouds linked to high aerosol loading (Fig. 1f, g), as well as the spatial distribution of latent heat anomalies (Fig. 2a, b). Comparative analysis shows that the evolution of precipitation during 9–11 July 2018 (Fig. S2b–d) is consistent with both the evolving distributions of ice-phase clouds (Fig. S2e–g) and the FLEXPART-simulated forward trajectories (Fig. S2h). As the episode progressed, most FLEXPART trajectories were transported at upper levels. Based on the FLEXPART simulations of ice-crystal transport, a simple scaling calculation estimates that approximately 45.68 % of the ice crystals generated over MQ can survive sublimation and sedimentation during transport over horizontal distances exceeding 1000 km and reach the free troposphere over eastern China, demonstrating the existence and importance of the downstream precipitation seeding effect associated with externally introduced aerosols activated in ice clouds over MQ.

From a physical perspective, one important mechanism within mid-latitude stratiform and mixed-phase cloud precipitation systems is the seeder-feeder mechanism, known to significantly enhance precipitation and thus play a criti-

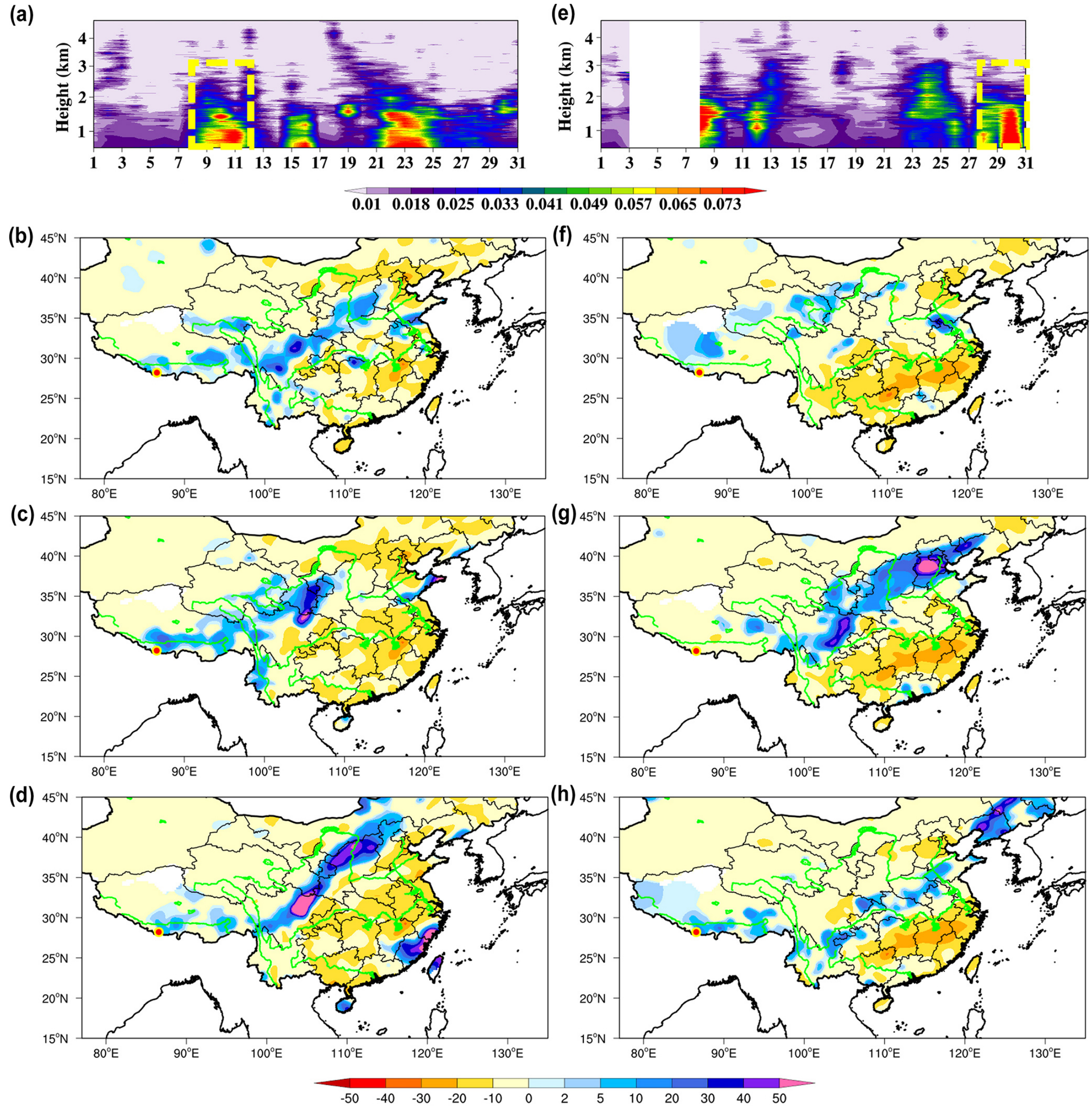

Figure 3. Temporal evolution of downstream precipitation responses: **(a, e)** Daily variations in AEC over MQ during **(a)** July 2018 and **(e)** July 2019 (Xu et al., 2025); yellow boxes denote selected high-aerosol events (9–11 July 2018; 28–30 July 2019). **(b–d, f–h)** Composite precipitation anomalies downstream on **(b, f)** the pollution day, **(c, g)** the second day, and **(d, h)** the third day following high-aerosol events for **(b–d)** July 2018 and **(f–h)** July 2019.

cal role in the Earth's water cycle (Purdy et al., 2005; He et al., 2015; Heymsfield et al., 2020). Seeder clouds, which can be pure ice or mixed-phase clouds themselves, produce ice crystals, for example supported by INPs, that fall into feeder clouds below (Ramelli et al., 2021). Feeder clouds, acting as a moisture reservoir, typically mainly consist of supercooled liquid cloud droplets that contribute to the growth of falling ice crystals or to an enhancement of particle number and ice mass (Hosler et al., 1957). The Wegener-Bergeron-Findeisen process (Wegener, 1911; Bergeron, 1935; Findeisen, 1938), where water vapor preferentially deposits onto ice crystals at the expense of supercooled droplets, accelerates ice growth and enhances precipitation. In this framework, upper-level ice crystals serve as precipitation embryos, while the abundant supercooled liquid water in the lower cloud layers provides the essential microphysical environment for their growth into precipitating hydrometeors. Xu et al. (2025) showed that, clouds influenced by aerosol activation exhibited more vigorous development. A comparison of the responses of convective-cloud development to tropospheric aerosols and water vapor indicated that convective-cloud development over the MQ region was primarily influenced by aerosol-induced ice clouds, as its response to water vapor was considerably weaker than that to AEC (Fig. 5 in

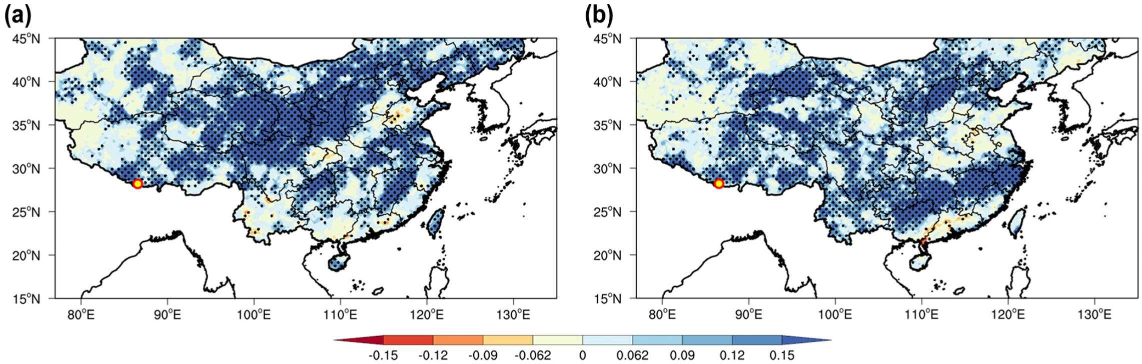

Figure 4. Relationship between ice-phase cloud occurrence and precipitation: **(a, b)** Spatial distributions of the Pearson correlation coefficient between ice-phase cloud frequency and hourly precipitation for **(a)** July 2018 and **(b)** July 2019; dotted regions indicate correlations statistically significant at the 95 % confidence level.

Xu et al., 2025). This further confirms the seeding effects of aerosol-activated ice clouds on downstream precipitation and the ice-crystal seeder–feeder mechanism as a key process governing the evolution of convective clouds with radar cross-section evidence of vertical coupling.

Based on satellite-derived cloud-phase data and ground-based aerosol lidar observations, we further quantify the relative contributions of different cloud phases under high and low aerosol conditions. Given that ice-phase clouds show the most pronounced enhancement under high aerosol loading (Fig. S1), we analyze the relationship between daily ice-phase cloud frequency and daily precipitation in the eastern TP downstream regions during July 2018 and July 2019. The results indicate that the identified high-impact downstream pathways correspond to regions with a strong positive correlation between ice-phase cloud occurrence and precipitation (Fig. 4a, b).

These findings provide additional evidence that high concentrations of transported aerosols over MQ enhance deep convective cloud development and facilitate the downstream transport of upper-level ice clouds, which can act as effective seeding agents to intensify cloud–precipitation cycling. This mechanism implies that increasing anthropogenic aerosol emissions in South Asia may not only activate deep convection over the southern TP but also modulate precipitation in downstream regions.

4 Conclusion

Using synergistic observation data from the STEP comprehensive vertical observation experiment concerning aerosol–cloud–precipitation interactions over MQ, to explore the impacts of South Asian aerosol inflow over MQ on downstream cloud-precipitation processes. The findings reveal that MQ exhibits high sensitivity to externally transported, high-concentration aerosols, which preferentially enhance ice-phase cloud formation and invigorate deep convective precipitation. The enhanced formation of ice-phase clouds leads to increased latent heat release, intensifying thermodynamic forcing over the TP and altering large-scale circulation patterns. Through long-range transport, aerosol-activated ice crystals are conveyed downstream, establishing a distinct "seeder–feeder"–type ice-cloud–precipitation conversion mechanism between upper- and lower-level clouds. A key discovery is that the upstream-downstream transmission is achieved via the long-range ice-crystal "seeding" effect. This process generates coherent downstream pathways characterized by enhanced ice-phase cloud occurrence, latent heat anomalies, and precipitation responses.

The identified downstream pathways vary interannually, reflecting differences in background circulation associated with the monsoon system and the subtropical high. These results reveal a previously underappreciated role of long-range aerosol transport in modulating cloud–precipitation coupling over the "Third Pole" and its downstream regions, and demonstrate that aerosols play a dual role in shaping precipitation patterns across the TP and China while exerting adverse impacts on human living environments. Enhanced South Asian aerosol transport may increase the likelihood of extreme rainfall events in downstream regions and contribute to uneven flood–drought conditions.

Taken together, these findings provide new physical insights into how increasing anthropogenic aerosols under climate change may influence regional precipitation patterns and hydrological processes across East Asia. They further suggest a potentially important, pathway through which enhanced South Asian aerosol transport may affect downstream extreme precipitation and environment change via aerosol-induced ice-phase cloud processes. Future work will explore and expand upon its quantitative mechanisms.

Code availability. The code developed for this study is available from the corresponding author on reasonable request.

Data availability. The continuous Lidar and X-band dual-polarization weather radar observation data used in this study were authorized and provided by the Anhui Institute of Optics and Fine Mechanics of Chinese Academy of Sciences and Chengdu Institute of Plateau Meteorology of China Meteorological Administration, respectively. Access to these datasets requires formal request submission to the corresponding author upon adherence to institutional data-sharing protocols regulating data usage. The hourly cloud phase full disk product of FY-4A/Advanced Geosynchronous Radiation Imager (AGRI) is provided by the National Satellite Meteorological Center, which can be found at https://data.nsmc.org.cn/DataPortal/cn/data/dataset.html (last access: 24 July 2025). Monthly aerosol optical depth (AOD) data at 550 nm from the MODIS Collection 6.1 product which can be found at https://giovanni.gsfc.nasa.gov/giovanni/ (last access: 9 June 2022). Observation data of common meteorological elements used in this study are derived from the Data Sets of Surface Meteorological Elements in China released by the National Meteorology Information Center, China Meteorological Administration, which can be found at http://data.cma.cn/ (last access: 22 May 2023). ERA5 is the fifth generation ECMWF reanalysis for the global climate and weather, which can be found at https://cds.climate.copernicus.eu/datasets/reanalysis-era5-pressure-levels-monthly-means?tab=overview (last access: 24 July 2025) and https://cds.climate.copernicus.eu/datasets/reanalysis-era5-pressure-levels?tab=overview (last access: 24 July 2025). FNL reanalysis data produced by the National Center for Environmental Prediction (NCEP)/National Center for Atmospheric Research (NCAR), which can be found at https://gdex.ucar.edu/datasets/d083002/ (last access: 23 May 2023).

Supplement. The supplement related to this article is available online at https://doi.org/10.5194/acp-26-13581-2026-supplement.

Author contributions. All the authors made contributions to this research and manuscript. XX and WC contributed equally to this research. XX, WC and TZ conceived and designed the project. CY, CW, KM, TZ, YL and SW collected the data. WC processed data and prepared most figures. ND prepared Fig. 3a and b. XX, WC and TZ analysed the study results and drafted the manuscript. All authors participated in scientific discussions, revised the manuscript, and approved the final version for publication.

Competing interests. The contact author has declared that none of the authors has any competing interests.

Disclaimer. Publisher's note: Copernicus Publications remains neutral with regard to jurisdictional claims made in the text, published maps, institutional affiliations, or any other geographical representation in this paper. The authors bear the ultimate responsibility for providing appropriate place names. Views expressed in the text are those of the authors and do not necessarily reflect the views of the publisher.

Acknowledgements. We deeply appreciate the National Observation and Research Station of China for Qomolangma Special Atmospheric Processes and Environmental Changes providing data support for this study.

Financial support. This research has been supported by the Second Tibetan Plateau Scientific Expedition and Research Program (STEP, grant no. 2019QZKK0105), Major Science and Technology Project of Tibet Autonomous Region (grant no. XZ202402ZD0006-06) and the National Natural Science Foundation of China (grant no. U2242208).

Review statement. This paper was edited by Shaocai Yu and reviewed by two anonymous referees.

References

Adhikari, P. and Mejia, J. F.: Influence of aerosols on clouds, precipitation and freezing level height over the foothills of the Himalayas during the Indian summer monsoon, Clim. Dynam., 57, 395–413, https://doi.org/10.1007/s00382-021-05710-2, 2021.

Bergeron, T.: On the physics of cloud and precipitation, in: Proceedings of the Fifth Assembly of the International Union of Geodesy and Geophysics, Lisbon, Portugal, IUGG, 156–178, 1935.

Cong, Z. Y., Kawamura, K., Kang, S. C., and Fu, P. Q.: Penetration of biomass-burning emissions from South Asia through the Himalayas: new insights from atmospheric organic acids, Sci. Rep., 5, 9580, https://doi.org/10.1038/srep09580, 2015.

de Leeuw, G., Sogacheva, L., Rodriguez, E., Kourtidis, K., Georgoulias, A. K., Alexandri, G., Amiridis, V., Proestakis, E., Marinou, E., Xue, Y., and van der A, R.: Two decades of satellite observations of AOD over mainland China using ATSR-2, AATSR and MODIS/Terra: data set evaluation and large-scale patterns, Atmos. Chem. Phys., 18, 1573–1592, https://doi.org/10.5194/acp-18-1573-2018, 2018.

Fan, J. W., Rosenfeld, D., Zhang, Y. W., Giangrande, S. E., Li, Z. Q., Machado, L. A. T., Martin, S. T., Yang, Y., Wang, J., Artaxo, P., Barbosa, H. M. J., Braga, R. C., Comstock, J. M., Feng, Z., Gao, W. H., Gomes, H. B., Mei, F., Pöhlker, C., Pöhlker, M. L., Pöschl, U., and de Souza, R. A. F.: Substantial convection and precipitation enhancements by ultrafine aerosol particles, Science, 359, 411–418, https://doi.org/10.1126/science.aan8461, 2018.

Fernald, F. G.: Analysis of atmospheric lidar observations: some comments, Appl. Opt., 23, 652–653, https://doi.org/10.1364/AO.23.000652, 1984.

Findeisen, W.: Die Kolloidmeterorologischem Vorgange der Niedershlagsbildung, Meteorol. Z., 55, 121–133, 1938.

Garrett, T. J. and Zhao, C. F.: Increased Arctic cloud longwave emissivity associated with pollution from mid-latitudes, Nature, 440, 787–789, https://doi.org/10.1038/nature04636, 2006.

Giorgi, F., Bi, X. Q., and Qian, Y.: Direct radiative forcing and regional climatic effects of anthropogenic aerosols over East Asia: a regional coupled climate-chemistry/aerosol model study, J. Geophys. Res., 107, 4439, https://doi.org/10.1029/2001JD001066, 2002.

Guo, J. P., Deng, M. J., Lee, S. S., Wang, F., Li, Z. Q., Zhai, P. M., Liu, H., Lv, W. T., Yao, W., and Li, X. W.: Delaying precipitation and lightning by air pollution over the Pearl River Delta. Part I: observational analyses, J. Geophys. Res.-Atmos., 121, 6472–6488, https://doi.org/10.1002/2015JD023257, 2016.

He, H., Gao, Q., Liu, X. E., Zhou, W., and Jia, X. C.: Numerical simulation of the structural characteristics and precipitation mechanism of stratiform clouds with embedded convections, Chin. J. Atmos. Sci., 39, 315–328, https://doi.org/10.3878/j.issn.1006-9895.1404.14102, 2015.

Heymsfield, A. J., Schmitt, C., Chen, C.-C.-J., Bansemer, A., Gettelman, A., Field, P. R., and Liu, C. T.: Contributions of the liquid and ice phases to global surface precipitation: observations and global climate modeling, J. Atmos. Sci., 77, 2629–2648, https://doi.org/10.1175/JAS-D-19-0352.1, 2020.

Hindman, E. E. and Upadhyay, B. P.: Air pollution transport in the Himalayas of Nepal and Tibet during the 1995–1996 dry season, Atmos. Environ., 36, 727–739, https://doi.org/10.1016/S1352-2310(01)00495-2, 2002.

Hosler, C. L., Jensen, D. C., and Goldshlak, L.: On the aggregation of ice crystals to form snow, J. Atmos. Sci., 14, 415–420, https://doi.org/10.1175/1520-0469(1957)014<0415:OTAOIC>2.0.CO;2, 1957.

Hua, S., Liu, Y. Z., Luo, R., Shao, T. B., and Zhu, Q. Z.: Inconsistent aerosol indirect effects on water clouds and ice clouds over the Tibetan Plateau, Int. J. Climatol., 40, 3832–3848, https://doi.org/10.1002/joc.6430, 2020.

Huang, J. P., Minnis, P., Yi, Y. H., Tang, Q., Wang, X., Hu, Y. X., Liu, Z. Y., Ayers, K., Trepte, C., and Winker, D.: Summer dust aerosols detected from CALIPSO over the Tibetan Plateau, Geophys. Res. Lett., 34, L18805, https://doi.org/10.1029/2007GL029938, 2007.

Intergovernmental Panel on Climate Change (IPCC): Climate Change 2021 – The Physical Science Basis: Working Group I Contribution to the Sixth Assessment Report of the Intergovernmental Panel on Climate Change (1st edn.), Cambridge University Press, https://doi.org/10.1017/9781009157896, 2023.

Jiang, J., Zhou, T. J., Qian, Y., Li, C., Song, F. F., Li, H. M., Chen, X. L., Zhang, W. X., and Chen, Z. M.: Precipitation regime changes in High Mountain Asia driven by cleaner air, Nature, 623, 544–549, https://doi.org/10.1038/s41586-023-06619-y, 2023.

Kang, S. C., Zhang, Q. G., Qian, Y., Ji, Z. M., Li, C. L., Cong, Z. Y., Zhang, Y. L., Guo, J. M., Du, W. T., Huang, J., You, Q. L., Panday, A. K., Rupakheti, M., Chen, D. L., Gustafsson, Ö., Thiemens, M. H., and Qin, D. H.: Linking atmospheric pollution to cryospheric change in the Third Pole region: current progress and future prospects, Natl. Sci. Rev., 6, 796–809, https://doi.org/10.1093/nsr/nwz031, 2019.

Khain, A., Rosenfeld, D., and Pokrovsky, A. A.: Aerosol impact on the dynamics and microphysics of deep convective clouds, Q. J. Roy. Meteor. Soc., 131, 2639–2663, https://doi.org/10.1256/qj.04.62, 2005.

Lau, K. M., Ramanathan, V., Wu, G. X., Li, Z., Tsay, S. C., Hsu, C., Sikka, R., Holben, B., Lu, D., Tartari, G., Chin, M., Koudelova, P., Chen, H., Ma, Y., Huang, J., Taniguchi, K., and Zhang, R.: The joint aerosol-monsoon experiment: a new challenge for monsoon climate research, Bull. Am. Meteorol. Soc., 89, 369–383, https://doi.org/10.1175/BAMS-89-3-369, 2008.

Lawrence, M. G.: Asia under a high-level brown cloud, Nat. Geosci., 4, 352–353, https://doi.org/10.1038/ngeo1166, 2011.

Levin, Z. and Cotton, W. R.: Aerosol Pollution Impact on Precipitation: A Scientific Review, Springer, https://doi.org/10.1007/978-1-4020-8690-8, 2009.

Levy, R. C., Mattoo, S., Munchak, L. A., Remer, L. A., Sayer, A. M., Patadia, F., and Hsu, N. C.: The Collection 6 MODIS aerosol products over land and ocean, Atmos. Meas. Tech., 6, 2989–3034, https://doi.org/10.5194/amt-6-2989-2013, 2013.

Li, X. F., Kang, S. C., Sprenger, M., Zhang, Y. L., He, X. B., Zhang, G. S., Tripathee, L., Li, C. L., and Cao, J. J.: Black carbon and mineral dust on two glaciers on the central Tibetan Plateau: sources and implications, J. Glaciol., 66, 1–11, https://doi.org/10.1017/jog.2019.100, 2020.

Liu, X. D., Xie, X. N., Yin, Z. Y., Liu, C. H., and Gettelman, A.: A modeling study of the effects of aerosols on clouds and precipitation over East Asia, Theor. Appl. Climatol., 106, 343–354, https://doi.org/10.1007/s00704-011-0436-6, 2011.

Liu, Y., Sato, Y., Jia, R., Xie, Y., Huang, J., and Nakajima, T.: Modeling study on the transport of summer dust and anthropogenic aerosols over the Tibetan Plateau, Atmos. Chem. Phys., 15, 12581–12594, https://doi.org/10.5194/acp-15-12581-2015, 2015.

Liu, Y. Z., Hua, S., Jia, R., and Huang, J. P.: Effect of aerosols on the ice cloud properties over the Tibetan Plateau, J. Geophys. Res.-Atmos., 124, 9594–9608, https://doi.org/10.1029/2019JD030463, 2019.

Liu, Y. Z., Li, Y. H., Huang, J. P., Zhu, Q. Z., and Wang, S. S.: Attribution of the Tibetan Plateau to northern drought, Natl. Sci. Rev., 7, 489–492, https://doi.org/10.1093/nsr/nwz191, 2020a.

Liu, Y. Z., Shao, T. B., Hua, S., Zhu, Q. Z., and Luo, R.: Association of anthropogenic aerosols with subtropical drought in East Asia, Int. J. Climatol., 40, 3500–3513, https://doi.org/10.1002/joc.6410, 2020b.

Liu, Y. Z., Huang, J. P., Wang, T. H., Li, J. M., Yan, H. R., and He, Y. L.: Aerosol-cloud interactions over the Tibetan Plateau: an overview, Earth Sci. Rev., 234, 104216, https://doi.org/10.1016/j.earscirev.2022.104216, 2022.

Liu, Z. Y. and Sugimoto, N.: Simulation study for cloud detection with space lidars by use of analog detection photomultiplier tubes, Appl. Opt., 41, 1750–1759, https://doi.org/10.1364/AO.41.001750, 2002.

Lohmann, U. and Feichter, J.: Global indirect aerosol effects: a review, Atmos. Chem. Phys., 5, 715–737, https://doi.org/10.5194/acp-5-715-2005, 2005.

Luo, M., Liu, Y. Z., Zhu, Q. Z., Tang, Y. H., and Alam, K.: Role and mechanisms of black carbon affecting water vapor transport to Tibet, Remote Sens., 12, 231, https://doi.org/10.3390/rs12020231, 2020.

Ma, Y. M., Xie, Z. P., Ma, W. Q., Han, C. B., Sun, F. L., Sun, G. H., Liu, L., Lai, Y., Wang, B. B., Liu, X., Zhao, W. Q., Ma, W. Y., Wang, F. F., Sun, L. J., Ma, B., Han, Y. Z., Wang, Z. Y., and Xi, Z. H.: QOMS: a comprehensive observation station for climate change research on the top of Earth, Bull. Am. Meteorol. Soc., 104, E563–E584, https://doi.org/10.1175/BAMS-D-22-0084.1, 2023.

Menon, S., Hansen, J., Nazarenko, L., and Luo, Y.: Climate effects of black carbon aerosols in China and India, Science, 297, 2250–2253, https://doi.org/10.1126/science.1075159, 2002.

Miao, Q. J., Xu, X. D., and Zhang X. J.: Characteristics of teleconnection wave train for circulation pattern of flood/drought in the middle and lower reaches of yangtze river and sea surface temperature over equatorial eastern pacific, Acta Meteorol. Sin., 60, 688–697, https://doi.org/10.11676/qxxb2002.082, 2002 (in Chinese).

Ming, J., Xiao, C. D., Du, Z. C., and Yang, X. G.: An overview of black carbon deposition in High Asia glaciers and its impacts on radiation balance, Adv. Water Resour., 55, 80–87, https://doi.org/10.1016/j.advwatres.2012.05.015, 2013.

Murray, B. J., O'Sullivan, D., Atkinson, J. D., and Webb, M. E.: Ice nucleation by particles immersed in supercooled cloud droplets, Chem. Soc. Rev., 41, 6519–6554, https://doi.org/10.1039/c2cs35200a, 2012.

Penner, J. E., Hegg, D., and Leaitch, R.: Unraveling the role of aerosols in climate change, Environ. Sci. Technol., 35, 332A–340A, https://doi.org/10.1021/es0124414, 2001.

Purdy, J. C., Austin, G. L., Seed, A. W., and Cluckie, I. D.: Radar evidence of orographic enhancement due to the seeder feeder mechanism, Meteorol. Appl., 12, 199–206, https://doi.org/10.1017/S1350482705001672, 2005.

Qian, Y., Gong, D. Y., Fan, J. W., Leung, L. R., Bennartz, R., Chen, D. L., and Wang, W. G.: Heavy pollution suppresses light rain in China: observations and modeling, J. Geophys. Res., 114, D00K02, https://doi.org/10.1029/2008JD011575, 2009.

Ramanathan, V., Chung, C., Kim, D., Bettge, T., Buja, L., Kiehl, J. T., Washington, W. M., Fu, Q., Sikka, D. R., and Wild, M.: Atmospheric brown clouds: Impacts on South Asian climate and hydrological cycle, Proc. Natl. Acad. Sci. USA, 102, 5326–5333, https://doi.org/10.1073/pnas.0500656102, 2005.

Ramelli, F., Henneberger, J., David, R. O., Bühl, J., Radenz, M., Seifert, P., Wieder, J., Lauber, A., Pasquier, J. T., Engelmann, R., Mignani, C., Hervo, M., and Lohmann, U.: Microphysical investigation of the seeder and feeder region of an Alpine mixed-phase cloud, Atmos. Chem. Phys., 21, 6681–6706, https://doi.org/10.5194/acp-21-6681-2021, 2021.

Rosenfeld, D.: Aerosols, clouds, and climate, Science, 312, 1323–1324, https://doi.org/10.1126/science.1128972, 2006.

Rosenfeld, D., Sherwood, S., Wood, R., and Donner, L.: Climate effects of aerosol-cloud interactions, Science, 343, 379–380, https://doi.org/10.1126/science.1247490, 2014.

Sayer, A. M., Munchak, L. A., Hsu, N. C., Levy, R. C., Bettenhausen, C., and Jeong, M.-J.: MODIS collection 6 aerosol products: comparison between aqua's e-deep blue, dark target, and "merged" data sets, and usage recommendations, J. Geophys. Res.-Atmos., 119, 13965–13989, https://doi.org/10.1002/2014JD022453, 2014.

Stohl, A., Forster, C., Frank, A., Seibert, P., and Wotawa, G.: Technical note: The Lagrangian particle dispersion model FLEXPART version 6.2, Atmos. Chem. Phys., 5, 2461–2474, https://doi.org/10.5194/acp-5-2461-2005, 2005.

Twomey, S.: The influence of pollution on the shortwave albedo of clouds, J. Atmos. Sci., 34, 1149–1152, https://doi.org/10.1175/1520-0469(1977)034<1149:tiopot>2.0.co;2, 1977.

Twomey, S. A., Piepgrass, M., and Wolfe, T. L.: An assessment of the impact of pollution on global cloud albedo, Tellus B, 36, 356–366, https://doi.org/10.3402/tellusb.v36i5.14916, 1984.

Wan, B. C., Gao, Z. Q., Chen, F., and Lu, C. G.: Impact of Tibetan Plateau surface heating on persistent extreme precipitation events in southeastern China, Mon. Weather Rev., 145, 3485–3505, https://doi.org/10.1175/MWR-D-17-0061.1, 2017.

Wang, C., Wu, C., and Li, L. P.: Data quality analysis and control method of X-band dual polarization radar, Plateau Meteorology, 38, 636–649, https://doi.org/10.7522/j.issn.1000-0534.2018.00096, 2019.

Wang, T. H., Chen, Y. X., Gan, Z. W., Han, Y., Li, J. M., and Huang, J. P.: Assessment of dominating aerosol properties and their long-term trend in the Pan-Third Pole region: a study with 10-year multi-sensor measurements, Atmos. Environ., 239, 117738, https://doi.org/10.1016/j.atmosenv.2020.117738, 2020.

Wegener, A.: Thermodynamik der Atmosphäre, J. A. Barth, Leipzig, 331 pp., https://doi.org/10.1038/090031a0, 1911.

Xiang, Y., Lv, L. H., Chai, W. X., Zhang, T. S., Liu, J. G., and Liu, W. Q.: Using Lidar technology to assess regional air pollution and improve estimates of PM2.5 transport in the North China Plain, Environ. Res. Lett., 15, 094071, https://doi.org/10.1088/1748-9326/ab9cfd, 2012.

Xiang, Y., Lv, L. H., Chai, W. X., Zhang, T. S., Liu, J. G., and Liu, W. Q.: Using Lidar technology to assess regional air pollution and improve estimates of $PM_{2.5}$ transport in the North China Plain, Environ. Res. Lett., 15, 094071, https://doi.org/10.1088/1748-9326/ab9cfd, 2020.

Xiang, Y., Zhang, T. S., Liu, J. G., Wan, X., Loewen, M., Chen, X. T., Kang, S. C., Fu, Y. B., Lv, L. H., Liu, W. Q., and Cong, Z. Y.: Vertical profile of aerosols in the Himalayas revealed by lidar: new insights into their seasonal/diurnal patterns, sources, and transport, Environ. Pollut., 285, 117686, https://doi.org/10.1016/j.envpol.2021.117686, 2021.

Xiao, Y. J., Wang, B., Chen, X. H., Cao, J. W., and Yang, X. M.: Differential Phase Data Quality Control of Mobile X-Band Dual-Polarimetric Doppler Weather Radar, Plateau Meteorology, 31, 223–230, 2012.

Xu, X. D. and Chen, L. S.: Advances of the Study on Tibetan Plateau Experiment of Atmospheric Sciences, J. Appl. Meteor. Sci., 17, 756–772, 2006 (in Chinese).

Xu, X. D., Zhou, M. Y., Chen, J. Y., Bian, L. G., Zhang, G. Z., Liu, H. Z., Li, S. M., Zhang, H. S., Zhao, Y. J., Dorje, S., and Wang, J. Z.: A comprehensive physical image of land-air dynamic and thermal structure on the Tibetan plateau, Sci. China Ser. D, 31, 428–440, https://doi.org/10.1360/02yd9060, 2001.

Xu, X. D., Tao, S. Y., Wang, J. Z., Chen, L. S., Zhou, L., and Wang, X. R.: The relationship between water vapor transport features of Tibetan plateau-monsoon "large triangle" affecting region and drought-flood abnormality of China, Acta Meteorol. Sin., 60, 257–266, https://doi.org/10.11676/qxxb2002.032, 2002.

Xu, X. D., Cai, W. Y., Zhao, T. L., Zhang, H., Guo, X. L., Liu, W. Q., Zhang, T. S., Zhao, R. Z., Wu, C., Li, Y. Q., Wang, L., Yan, P., and Yang, C. J.: Understanding clouds and precipitation over the Mount Qomolangma: how does the aerosol activation effect exist?, Sci. Bull., 70, 3649–3658, https://doi.org/10.1016/j.scib.2025.09.031, 2025.

Ying, T., Li, J., Jiang, Z. J., Liu, G. Y., Zhang, Z. Y., Zhang, L., Dong, Y. M., and Zhao, C. F.: Increased aerosol scattering contributes to the recent monsoon rainfall decrease over the Gangetic Plain, Sci. Bull., 68, 2629–2638, https://doi.org/10.1016/j.scib.2023.08.052, 2023.

Zhang, H., Wang, Z. L., and Zhao, S. Y.: Atmospheric aerosol and its climate effect, in: 1st edn., China Meteorological Press, Beijing, ISBN 978-7-5029-6676-8, 2017 (in Chinese).

Zhao, C. F., Yang, Y. K., Fan, H., Huang, J. P., Fu, Y. F., Zhang, X. Y., Kang, S. C., Cong, Z. Y., Letu, H., and Menenti, M.: Aerosol characteristics and impacts on weather and climate over the Tibetan Plateau, Natl. Sci. Rev., 7, 492–495, https://doi.org/10.1093/nsr/nwz184, 2020.

Zhao, C. F., Sun, Y., Yang, J., Li, J. F., Zhou, Y., Yang, Y. K., Fan, H., and Zhao, X.: Observational evidence and mechanisms of aerosol effects on precipitation, Sci. Bull., 69, 1569–1580, https://doi.org/10.1016/j.scib.2024.03.014, 2024.

Zhao, C. F., Li, J. F., and Yang, Y. K.: A short review of microphysical effects of aerosols on clouds and precipitation, Chin. J. Atmos. Sci., 49, 949–963, https://doi.org/10.3878/j.issn.1006-9895.2503.25015, 2025.

Zhou, X., Bei, N., Liu, H., Cao, J., Xing, L., Lei, W., Molina, L. T., and Li, G.: Aerosol effects on the development of cumulus clouds over the Tibetan Plateau, Atmos. Chem. Phys., 17, 7423–7434, https://doi.org/10.5194/acp-17-7423-2017, 2017.

Zhu, S. Z., Qian, L., Ma, X. Q., Qiu, Y. J., Yang, J., He, X., Li, J. J., Zhu, L., Gong, J., and Lu, C. S.: Impact of Aerosols on the Macrophysical and Microphysical Characteristics of Ice-Phase and Mixed-Phase Clouds over the Tibetan Plateau, Remote Sens., 16, 1781, https://doi.org/10.3390/rs16101781, 2024.

Zhuo, G., Xu, X. D., and Chen, L. S.: Instability of eastward movement and development of convective cloud clusters over Tibetan Plateau, J. Appl. Meteor. Sci., 13, 447–456, 2002 (in Chinese).